

TABLE I  
ULTRAVIOLET AND VISIBLE SPECTRAL DATA IN ACETONITRILE

Compound	$\lambda_{\max}$ , m $\mu$ (cm <sup>-1</sup> )	$\epsilon$
MoOCl <sub>3</sub> ·OMPA	240 (41,700)	4870
	306 (32,700)	2900
	447 (22,400)	43
	732 (13,650)	21

<sup>2</sup>B<sub>2</sub> → <sup>2</sup>E(1) and <sup>2</sup>B<sub>2</sub> → <sup>2</sup>B<sub>1</sub>. The bands at 32,700 and 41,700 cm<sup>-1</sup> are charge-transfer bands, as indicated by their high molar absorptivities.

The Mo=O stretching frequency appears at 990 cm<sup>-1</sup> in MoOCl<sub>3</sub>·OMPA, which is slightly higher than Mo=O stretching frequencies previously reported.<sup>6</sup> These include 965 cm<sup>-1</sup> for [MoOCl<sub>5</sub>]<sup>2-</sup>, 979 cm<sup>-1</sup> for MoOCl<sub>3</sub>·bipy, 967 cm<sup>-1</sup> for MoOCl<sub>3</sub>·2(C<sub>6</sub>H<sub>5</sub>)<sub>3</sub>PO, and 980 cm<sup>-1</sup> for MoOCl<sub>3</sub>·2CH<sub>3</sub>CN. The decrease in the P=O stretching frequency and the increase in the P—N stretching frequencies are support for coordination of molybdenum with the phosphoryl oxygens. In conclusion, the experimental evidence supports the presence of six-coordinate molybdenum in a molecular complex in which [Mo=O]<sup>3+</sup> is attached to three chlorides and two phosphoryl oxygens.

**UO<sub>2</sub>(ClO<sub>4</sub>)<sub>2</sub>·3OMPA.**—At present, there is general agreement that UO<sub>2</sub><sup>2+</sup> can form complexes with four, five, and six donor sites.<sup>10</sup> The molar conductance of UO<sub>2</sub>(ClO<sub>4</sub>)<sub>2</sub>·3OMPA in nitromethane is in the range expected for 2:1 electrolytes.<sup>11</sup> The shifts in the P=O and P—N stretching frequencies (Table II) are in the direction expected for formation of chelate rings through the phosphoryl oxygens. It was not possible to assign a U=O stretching frequency since this occurs in the same region as P—N<sub>1</sub> (900–1000 cm<sup>-1</sup>). On the basis of these experimental data, a likely structure for UO<sub>2</sub>(ClO<sub>4</sub>)<sub>2</sub>·3OMPA is one in which the phosphoryl oxygens from the OMPA molecules form chelate rings in

TABLE II  
INFRARED SPECTRAL ASSIGNMENTS (CM<sup>-1</sup>)<sup>a</sup>

Band	OMPA	Th(ClO <sub>4</sub> ) <sub>4</sub> · 4OMPA <sup>b</sup>	UO <sub>2</sub> (ClO <sub>4</sub> ) <sub>2</sub> · 3OMPA <sup>c</sup>	MoOCl <sub>3</sub> · OMPA <sup>c</sup>
P=O	1238 s	1140 s	1160 s, 1185 sh	1188 s
P—N <sub>1</sub>	988 s	995 s	1000 s	1018 m
P—N <sub>2</sub>	756 w	790, 765 w	795 w, 770 m, 775 m	795 w
P—O—P	915 s	905 s	920 s	910 s
Metal—O	...	...	...	990 s
ClO <sub>4</sub> <sup>-</sup>	...	1090 s	1090 s	...

<sup>a</sup> Intensities of bands: s, strong; m, medium; w, weak; sh, shoulder. <sup>b</sup> KBr pellet. <sup>c</sup> Nujol mull.

the equatorial positions around [O=U=O]<sup>2+</sup>. This would give a structure similar to that found for NaUO<sub>2</sub>(C<sub>2</sub>H<sub>3</sub>O<sub>2</sub>)<sub>3</sub><sup>12</sup> except that the chelate rings involving OMPA molecules would be puckered.

**Th(ClO<sub>4</sub>)<sub>4</sub>·4OMPA.**—The elemental analysis, infrared spectral data, and conductivity measurements support the assignment of a coordination number of eight to Th<sup>4+</sup>. The decrease in the P=O stretching frequency (98 cm<sup>-1</sup>) as well as the increase in P—N<sub>1</sub> and P—N<sub>2</sub> stretching frequencies are support for co-

ordination of the Th<sup>4+</sup> to the phosphoryl oxygens of OMPA.

The acetylacetonate (acac) complex of Th<sup>4+</sup>, Th(acac)<sub>4</sub>, has an Archimedian antiprismatic structure.<sup>13</sup> The ability of OMPA to coordinate as a bidentate ligand and the similarity in stoichiometry and ring size in the systems Th(ClO<sub>4</sub>)<sub>2</sub>·4OMPA and Th(acac)<sub>4</sub> lead us to predict an Archimedian antiprismatic structure for Th(ClO<sub>4</sub>)<sub>4</sub>·4OMPA.

(13) D. Grdenic and B. Matkovic, *Nature*, **182**, 465 (1958).

CONTRIBUTION FROM THE DIVISION OF ENGINEERING  
AND THE DEPARTMENT OF CHEMISTRY,  
BROWN UNIVERSITY, PROVIDENCE, RHODE ISLAND 02912

## The Preparation and Electrical Properties of Niobium Selenide and Tungsten Selenide<sup>1</sup>

By R. KERSHAW, M. VLASSE, AND A. WOLD

Received February 27, 1967

Revolinsky, *et al.*,<sup>2</sup> have shown that NbSe<sub>2</sub> has both a hexagonal two-layer structure of the NbS<sub>2</sub> type and a four-layer structure of a new structure type. The structures are composed of trigonal prismatic NbSe<sub>2</sub> slabs.

The anions are arranged as two parallel close-packed sheets with the metal atoms occupying trigonal prismatic sites. The arrangement of the cations with respect to each other is that of a close-packed hexagonal layer. The NbSe<sub>2</sub> slabs can be stacked in a number of different ways with one, two, three, four, or six NbSe<sub>2</sub> layer sequences being the usual arrangements. Figure 1a illustrates the two-layer sequence for NbSe<sub>2</sub>. For both the two-layer ( $\epsilon$ ) and the four-layer ( $\zeta$ ) structures, the coordination within the "molecular" slabs is trigonal prismatic.

Beerntsen, *et al.*,<sup>3</sup> have shown that the two-layer NbSe<sub>2</sub> structure is superconducting. The high-temperature four-layer modification was also superconducting. Revolinsky, *et al.*,<sup>2</sup> reported that the superconducting transition temperature for the two-layer phase was 7°K.

Brixner<sup>4</sup> has described the preparation, structure, and thermoelectric properties of WSe<sub>2</sub>. WSe<sub>2</sub> is a rather well-behaved semiconductor with a relatively low electrical conductivity (increasing with temperature) and a high Seebeck coefficient. Figure 1b shows a two-layer sequence for WSe<sub>2</sub>. Both WSe<sub>2</sub> and NbSe<sub>2</sub> crystallize in the D<sub>6h</sub><sup>4</sup>-P6/mmc space group and have exactly the same anion packing. It can be seen from Figure 1 that only the cation arrangement differs.

(1) This work has been supported by ARPA and Grant No. AF 33(615)-3844.

(2) E. Revolinsky, G. A. Spiering, and D. J. Beerntsen, *J. Phys. Chem. Solids*, **26**, 1029 (1965).

(3) D. J. Beerntsen, G. A. Spiering, and C. H. Armitage, *IEEE Trans. Aerospace*, **2**, 816 (1964).

(4) L. H. Brixner, *J. Inorg. Nucl. Chem.*, **24**, 257 (1962).

(10) A. E. Comyns, *Chem. Rev.*, **60**, 115 (1960).

(11) N. S. Gill and R. S. Nyholm, *J. Chem. Soc.*, 3997 (1959).

(12) W. H. Zachariasen and H. A. Plettinger, *Acta Cryst.*, **12**, 526 (1959).

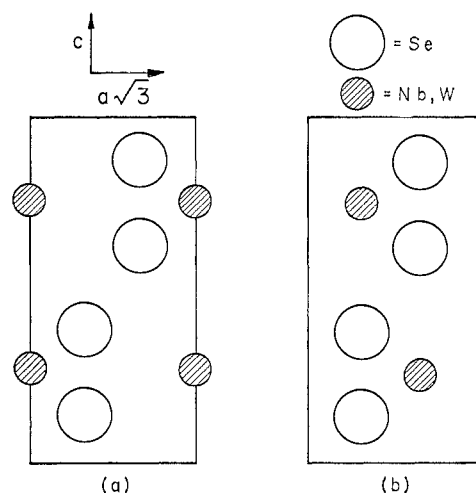


Figure 1.—Sections through the  $(11\bar{2}0)$  planes of (a) the hexagonal two-layer  $\epsilon$  phase of  $\text{NbSe}_2$  and (b) hexagonal  $\text{WSe}_2$ .

Tungsten(IV) selenide was found to be a p-type semiconductor with a resistivity of  $7.2 \times 10^{-1}$  ohm cm at  $25^\circ$  and  $1.2 \times 10^3$  ohm cm at  $-196^\circ$ . Tantalum-substituted p-type  $\text{WSe}_2$  had the best thermoelectric properties with a figure of merit about  $0.5 \times 10^{-3} \text{ deg}^{-1}$  from 500 to  $1000^\circ$ .

The electrical properties reported by Revolinsky, *et al.*, and Brixner on  $\text{NbSe}_2$  and  $\text{WSe}_2$  were measured on polycrystalline samples. In order to study further the interesting transport properties of these compounds, it was the intention of this study to prepare well-characterized single crystals of both selenides and to determine their structural and electrical properties. Single crystals of  $\text{NbSe}_2$  and  $\text{WSe}_2$  have been grown by the chemical-transport method<sup>4</sup> using iodine or bromine as the transporting agent. However, the electrical properties for these compounds were not measured on single crystals. This may have been because the crystals grown were thin and friable. Large, homogeneous, well-formed crystals of  $\text{NbSe}_2$  and  $\text{WSe}_2$  were grown for this study by a modification of Brixner's procedure. The electrical conductivity of both compounds was measured on single-crystal specimens and the results were compared with those of previous investigators.

#### Experimental Section

**Preparation.**—Niobium(IV) and tungsten(IV) selenides were prepared by allowing the elements<sup>5</sup> to react in evacuated (less than  $10^{-3}$  torr) silica tubes. The tubes were heated at  $15^\circ/\text{hr}$  to  $600^\circ$  and then held at temperature for 4 days. The samples were opened in a drybox, ground in an agate mortar, and resealed in silica tubes. The samples were refired for 4 days at  $600^\circ$  for  $\text{NbSe}_2$  and  $800^\circ$  for  $\text{WSe}_2$ . All lines in the X-ray diffraction patterns of the products were indexed on the basis of a hexagonal unit cell. For  $\text{NbSe}_2$   $a = 3.446 \pm 0.005$  and  $c = 12.55 \pm 0.01$  Å, for  $\text{WSe}_2$   $a = 3.290 \pm 0.005$  and  $c = 12.97 \pm 0.01$  Å. Chemical analyses indicated the compositions of the selenides to be  $\text{NbSe}_{1.994}$  and  $\text{WSe}_{2.005}$ . Analysis of the powders was done by igniting the selenide at  $800^\circ$ , in a stream of dry oxygen, to either  $\text{Nb}_2\text{O}_5$  or  $\text{WO}_3$ .

Large single crystals of  $\text{NbSe}_2$  and  $\text{WSe}_2$  were prepared by chemical transport using a concentration of  $5 \text{ mg}/\text{cm}^3$  of iodine as the transporting agent. The iodine used was resublimed under vacuum and dried 1 week over  $\text{P}_2\text{O}_5$ . A melting point capillary was filled with the calculated weight of iodine, sealed at a low pressure of  $10^{-3}$  torr, and placed in the filling apparatus shown in Figure 2. The charge powder was added through a long-stemmed funnel, the apparatus was sealed to a vacuum system and evacuated to a pressure of less than  $10^{-6}$  torr. The charge was outgassed at  $150^\circ$  for 3 hr and the apparatus was sealed off from the system. The weight is swung against the capillary to break it, and the iodine is sublimed onto the charge. The transport tube is then sealed off to a length of approximately 11 in. The tube containing the iodine and selenide charge is placed in the furnace. Preliminary experiments showed that a two-zone furnace, as ordinarily used, would not yield crystals of the necessary size and perfection. A three-zone furnace having an auxiliary heater after the growth (center) zone was constructed. The temperature profile of the furnace was adjusted by varying the temperature of this auxiliary heater. The best crystals are produced when the temperature of the transport tube decreases smoothly over several inches from the charge end to the growth zone. The growth zone temperature is constant for 3 in. and then gradually increases toward the empty tip of the tube due to the auxiliary heater. This profile causes the coolest part of the tube, where the crystals grow, to be at the center of the tube, rather than the end. The crystals are therefore spread out and well formed, instead of being crowded into the tip of the tube.

At the start of the transport run, the charge end is kept at room temperature, the other end is maintained at  $875^\circ$ , and the center or growth zone is also kept at  $875^\circ$ . This arrangement of the temperature zones minimizes the number of nuclei in the growth (center) zone. After 24 hr the charge zone is raised to  $800^\circ$ , the other end is maintained at  $875^\circ$ , and the center zone is programmed to  $750^\circ$  at a rate of  $1^\circ/\text{hr}$  for the growth of  $\text{WSe}_2$  crystals. The growth zone is lowered to  $725^\circ$  for the growth of  $\text{NbSe}_2$  crystals. Transport is allowed to continue for 5 days after the growth zone reaches the desired temperature. All of the heaters are then shut off and the tube is allowed to cool to room temperature. Crystals in the form of thin plates with dimensions greater than  $5 \times 10 \text{ mm}$  were grown by this technique.

The crystals are removed from the transport tube by snapping it inside an evacuated rubber hose. Air is slowly bled in and the crystals are removed and washed with carbon tetrachloride to remove any excess iodine. Analysis of the crystals was done by igniting the selenide, in a stream of dry oxygen, to either  $\text{Nb}_2\text{O}_5$  or  $\text{WO}_3$ .

**Physical Measurements.**—Crystallographic parameters were determined on powder samples with a Norelco diffractometer using monochromatic radiation (AMR-202 focusing monochromator) and a high-intensity copper source. The dimensions of the cells were in agreement with those reported by previous investigators. These values were also confirmed by single-crystal analysis using precession X-ray techniques.

Electrical resistivity as a function of temperature was determined by means of standard four-probe dc measurements. Electrical contacts were made to the  $\text{WSe}_2$  crystals by the use of a gallium-tin solder, and a conducting silver paste was used for the  $\text{NbSe}_2$  crystals. The results of these measurements are shown in Figures 3 and 4. The resistivity data were taken on both heating and cooling cycles. No apparent hysteresis was observed. The measurements were reproducible with different crystals and with different points of contact on each crystal. Crystals from three different batches were measured.

There appears to be little substitution of selenium by iodine in these compounds. In attempts to prepare the compounds  $\text{WSe}_{1.99}\text{I}_{0.01}$  and  $\text{NbSe}_{1.99}\text{I}_{0.01}$  it was observed that appreciable iodine vapor was present in the silica reaction tubes after all the selenium reacted with the metal. In addition, the cell constants of the transported crystals were the same as that of the charge powder indicating no apparent anion substitution in the lattice.

(5) 99.9% niobium, 99.95% tungsten, and 99.9998% selenium were obtained from Gallard Schlesinger Co., New York, N. Y.

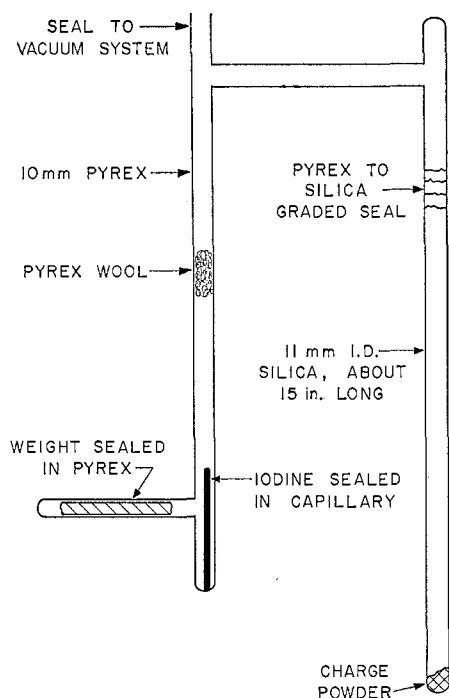


Figure 2.—Apparatus used to introduce iodine into the transport tube.

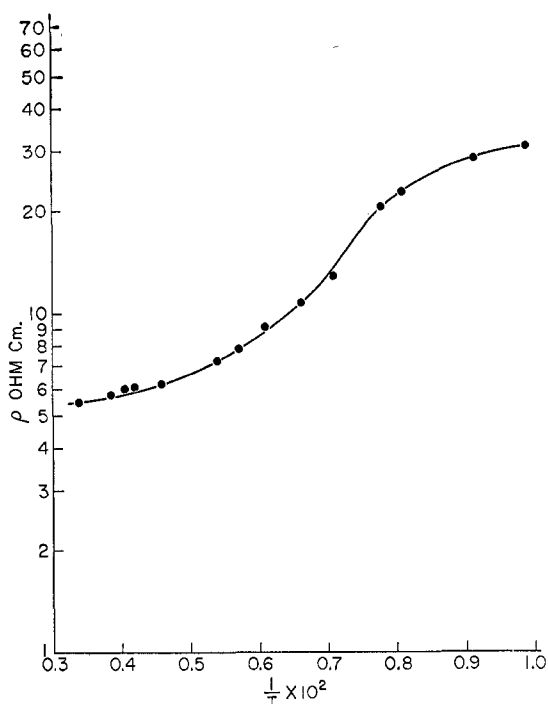


Figure 3.—Resistivity vs.  $100/T$  for  $WSe_2$ .

### Discussion

The procedure outlined in this study for the preparation of single crystals of  $NbSe_2$  and  $WSe_2$  is a marked improvement over the usual chemical-transport technique. The growth of large, well-formed selenide crystals required a gradual reduction of the growth zone temperature to less than that of the charge zone. The usual procedure is to set the zones at the desired temperatures after back transport of the nuclei has been carried out. The programming down of the

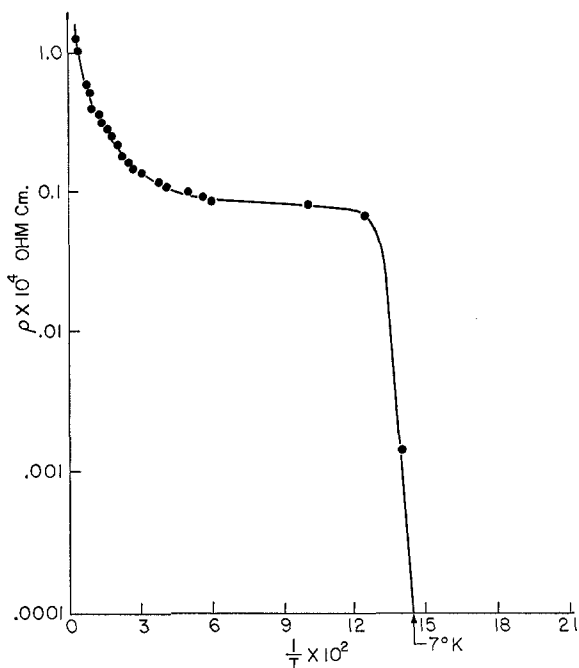


Figure 4.—Resistivity vs.  $100/T$  for  $NbSe_2$ .

growth zone temperature ensures the formation of a minimum number of nuclei. The growth of these relatively few nuclei depletes the vapor sufficiently, so that no new nuclei can form. Thus, all of the material transported deposits as a few large, well-formed crystals, rather than many small, intergrown ones. The slower initial rate of growth produces crystals that are homogeneous and contain fewer imperfections than those grown by other methods.

From Figures 3 and 4, it can be seen that  $NbSe_2$  shows metallic-like behavior, whereas  $WSe_2$  is a well-behaved semiconductor with a relatively low electrical conductivity. The superconducting transition for  $NbSe_2$ , measured on single crystals, takes place at  $7^\circ K$  which is in agreement with the value reported by Revolinsky, *et al.*,<sup>2</sup> for polycrystalline samples. Brixner<sup>4</sup> has indicated  $NbSe_2$  behaves as a metal because there is a free electron available for the conduction band, whereas for  $WSe_2$  the paired electrons are more difficult to promote to the conduction band. It may be possible to discuss the difference in the conductivity of  $NbSe_2$  and  $WSe_2$  in terms of a model proposed by Goodenough.<sup>6</sup> He has indicated that the formation of two types of bands is possible. First, certain of the d-wave functions can be broadened into bands, and, second, bands may also be formed between certain of the metal orbitals and the  $p_x$  orbitals of the selenium anions. For compounds with completely filled or empty bands, semiconductor behavior is observed, whereas partially filled bands give rise to metallic behavior. The manner in which the bands are formed and occupied in these compounds is presently under investigation by Goodenough.

**Acknowledgments.**—The authors wish to thank Mr. L. C. Upadhyayula for the conductivity measure-

(6) J. B. Goodenough, to be published.

ments of NbSe<sub>2</sub> and WSe<sub>2</sub> and the Air Force Systems Command of the Wright-Patterson Air Force Base and the Advanced Research Projects Agency for their financial support of the work.

CONTRIBUTION FROM THE CLINICAL LABORATORY, UNITED STATES NAVAL HOSPITAL, CAMP LEJEUNE, NORTH CAROLINA, AND THE DEPARTMENT OF SCIENCE, BLOOMSBURG STATE COLLEGE, BLOOMSBURG, PENNSYLVANIA

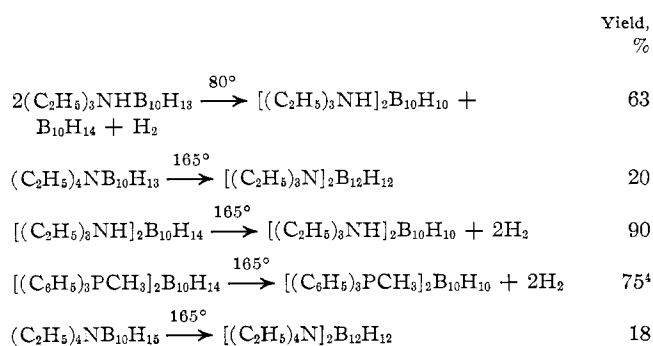
## Studies on Boron Hydrides. II.<sup>1</sup> Thermal Decomposition of Some Higher Hydroborates

BY ALLEN R. SIEDLE,<sup>2</sup> J. GRANT, AND M. D. TREBLOW

Received March 9, 1967

Recent reports<sup>3</sup> of the pyrolysis of B<sub>3</sub>H<sub>8</sub><sup>-</sup> to yield B<sub>12</sub>H<sub>12</sub><sup>2-</sup> prompt us to report some results with higher hydroborates.

The thermal decompositions listed below were demonstrated. Yields are expressed as weight per cent of



starting material recovered as product; if a balanced equation is given, they are calculated in the usual manner. The decomposition of (C<sub>2</sub>H<sub>5</sub>)<sub>3</sub>NHB<sub>10</sub>H<sub>13</sub> and of B<sub>10</sub>H<sub>14</sub><sup>2-</sup> salts also gave rise to small amounts of B<sub>12</sub>H<sub>12</sub><sup>2-</sup> salts.

The mechanisms of these reactions are obscure. The B<sub>10</sub>H<sub>15</sub><sup>-</sup> ion<sup>5</sup> very likely loses hydrogen to form B<sub>10</sub>H<sub>13</sub><sup>-</sup>,<sup>6,7</sup> which subsequently decomposes. This may occur by an autoprotolysis yielding decaborane, hydrogen, and the hypothetical B<sub>10</sub>H<sub>12</sub><sup>2-</sup>, which would be expected to rapidly eliminate hydrogen to form B<sub>10</sub>H<sub>10</sub><sup>2-</sup>. The B<sub>12</sub>H<sub>12</sub><sup>2-</sup> ion may arise in a number of ways as it is readily formed from many different hydroborates and boranes.<sup>3b</sup> Three possible modes

of its formation, no two of which are mutually exclusive, are combination of decaborane with either B<sub>10</sub>H<sub>10</sub><sup>3-</sup>,<sup>8</sup> a known<sup>3</sup> precursor of B<sub>12</sub>H<sub>12</sub><sup>2-</sup>, or alternatively with B<sub>10</sub>H<sub>13</sub><sup>-</sup> to form B<sub>11</sub>H<sub>14</sub><sup>-</sup>. Diborane and B<sub>10</sub>H<sub>13</sub><sup>-</sup> react to form B<sub>11</sub>H<sub>14</sub><sup>-</sup>,<sup>9</sup> which is converted by hydroborate to B<sub>12</sub>H<sub>12</sub><sup>2-</sup>;<sup>1,3b</sup> other boranes and hydroborates would likely be effective as well. The observation<sup>6</sup> that ethylene glycol dimethyl ether solutions of NaB<sub>10</sub>H<sub>13</sub> generate B<sub>11</sub>H<sub>14</sub><sup>-</sup> on standing at room temperature points to another source of this ion.

We have pyrolyzed (C<sub>2</sub>H<sub>5</sub>)<sub>3</sub>NHB<sub>10</sub>H<sub>9</sub>D<sub>4</sub>, prepared from 1,2,3,4-B<sub>10</sub>H<sub>10</sub>D<sub>4</sub>,<sup>10</sup> at 80° and examined the deuterium distribution in the resulting [(C<sub>2</sub>H<sub>5</sub>)<sub>3</sub>NH]<sub>2</sub>-B<sub>10</sub>H<sub>6</sub>D<sub>4</sub> by <sup>11</sup>B nuclear magnetic resonance spectroscopy. The stereospecificity of the reaction of 1,2,3,4-B<sub>10</sub>H<sub>10</sub>D<sub>4</sub> with triethylamine<sup>11</sup> was not observed; instead, the deuterium appeared to be statistically distributed between apical and equatorial positions.

Since the ions B<sub>10</sub>H<sub>10</sub><sup>2-</sup> and B<sub>12</sub>H<sub>12</sub><sup>2-</sup> may be regarded as highly resonance-stabilized structures, the above reactions are somewhat reminiscent of aromatization reactions in organic chemistry, the driving force here being the formation of a polyhedral hydroborate ion.

### Experimental Section

Starting materials were prepared according to literature methods. All reactions were run in a nitrogen atmosphere using dry solvents. In every case, product identity was established by all of the following methods: infrared<sup>12</sup> and <sup>11</sup>B nuclear magnetic resonance spectra<sup>12</sup> and X-ray powder patterns.

**Decomposition of Tridecahydrodecaborate(1-) Salts.**—A. A suspension of 0.5 g (2.2 mmoles) of (C<sub>2</sub>H<sub>5</sub>)<sub>3</sub>NHB<sub>10</sub>H<sub>13</sub><sup>13</sup> in 50 ml of benzene was refluxed and stirred overnight. On cooling, 0.22 g (0.69 mmole), 63%, of [(C<sub>2</sub>H<sub>5</sub>)<sub>3</sub>NH]<sub>2</sub>B<sub>10</sub>H<sub>10</sub> separated. It was filtered off and recrystallized from acetonitrile-methylene chloride. The X-ray powder pattern showed faint lines due to [(C<sub>2</sub>H<sub>5</sub>)<sub>3</sub>NH]<sub>2</sub>B<sub>12</sub>H<sub>12</sub>.

The above benzene filtrate was evaporated to dryness under reduced pressure to leave a yellow resin from which a small amount of decaborane, identified by its infrared spectrum, sublimed upon heating under vacuum.

B. A mixture of 1.56 g of (C<sub>2</sub>H<sub>5</sub>)<sub>4</sub>NB<sub>10</sub>H<sub>13</sub><sup>13</sup> and 50 ml of mesitylene was stirred under reflux overnight. The slurry was cooled to room temperature and filtered. The filter cake was washed with pentane and recrystallized three times from acetonitrile to yield 0.31 g of pure [(C<sub>2</sub>H<sub>5</sub>)<sub>4</sub>N]<sub>2</sub>B<sub>12</sub>H<sub>12</sub>.

**Decomposition of Tetradecahydrodecaborate(1-) Salts.** A. A mixture of 1.0 g (1.4 mmoles) of [(C<sub>6</sub>H<sub>5</sub>)<sub>3</sub>PCH<sub>3</sub>]<sub>2</sub>B<sub>10</sub>H<sub>14</sub><sup>14</sup> and 100 ml of mesitylene was refluxed and stirred for 24 hr. The solid phase was removed by filtration and recrystallized twice from acetonitrile to afford 0.75 g (1.05 mmoles), 75%, of [(C<sub>6</sub>H<sub>5</sub>)<sub>3</sub>PCH<sub>3</sub>]<sub>2</sub>B<sub>10</sub>H<sub>10</sub>. Nuclear magnetic resonance analysis indicated that this product contained about 5% of the B<sub>12</sub>H<sub>12</sub><sup>2-</sup> salt.

B. The triethylammonium salt of B<sub>10</sub>H<sub>14</sub><sup>2-</sup> was treated as above for 0.25 hr. Workup and recrystallization from acetonitrile-benzene afforded a 90% yield of the B<sub>10</sub>H<sub>10</sub><sup>2-</sup> salt. Its X-

(1) Part I: R. M. Adams, A. R. Siedle, and J. Grant, *Inorg. Chem.*, **3**, 461 (1964).

(2) Author to whom correspondence should be directed at U. S. Naval Hospital, Camp Lejeune, N. C.

(3) (a) I. A. Ellis, D. F. Gaines, and R. Schaeffer, *J. Am. Chem. Soc.*, **85**, 3885 (1963); (b) H. C. Miller, N. E. Miller, and E. L. Muettterties, *Inorg. Chem.*, **3**, 1456 (1964).

(4) R. Toeniskoetter, *Dissertation Abstr.*, **20**, 879 (1959), observed that Na<sub>2</sub>B<sub>10</sub>H<sub>14</sub> lost hydrogen on heating but the products of this reaction were not identified.

(5) J. A. Dupont and M. F. Hawthorne, *Chem. Ind. (London)*, 405 (1962).

(6) R. Schaeffer and F. Tebbe, *Inorg. Chem.*, **3**, 1638 (1964).

(7) A. R. Siedle, unpublished results.

(8) We wish to thank one of the referees for suggesting this possibility.

(9) V. D. Aftandilian, H. C. Miller, G. W. Parshall, and E. L. Muettterties, *Inorg. Chem.*, **1**, 734 (1962).

(10) J. A. Dupont and M. F. Hawthorne, *J. Am. Chem. Soc.*, **84**, 804 (1962).

(11) A. R. Pitochelli, R. Ettinger, J. A. Dupont, and M. F. Hawthorne, *ibid.*, **84**, 1057 (1962).

(12) E. L. Muettterties, J. T. Balthis, Y. T. Chia, W. H. Knoth, and H. C. Miller, *Inorg. Chem.*, **3**, 444 (1964).

(13) M. F. Hawthorne, A. R. Pitochelli, D. Strahm, and J. Miller, *J. Am. Chem. Soc.*, **82**, 1825 (1960).

(14) E. L. Muettterties, *Inorg. Chem.*, **2**, 647 (1963).